Lipid-Based Liquid Crystalline Nanoparticles Facilitate Cytosolic Delivery of siRNA *via* Structural Transformation

Shufang He,[†,‡] Weiwei Fan,[†,‡] Na Wu,[†] Jingjing Zhu,[†] Yunqiu Miao,[†] Xiaran Miao,[§] Feifei Li,[†] Xinxin Zhang,[†,*] Yong Gan,[†,*]

Supporting Information

MATERIALS AND METHODS

Materials. Purified mouse anti-EEA1 was purchased from BD Biosciences. Mouse monoclonal CDK1 antibody was purchased from Abcam Inc. LAMP1 (D2D11) XP® rabbit mAb was purchased from Cell Signaling Technology, Inc. Trizol, Lipofectamine™ 2000 and Alexa-647 labeled Dextran were purchased from Invitrogen Life Techonologies. Loading buffer, PrimeScript™ RT Reagent Kit and SYBR® Premix Ex Taq™ II were obtained from Takara Biotechnology Co., Ltd. ATP detection kit was purchased from Promega. RIPA lysis buffer, DiO perchlorate, DiI perchlorate, DAPI dihydrochloride, Hoechst 33258, Alexa 555 labelled donkey anti-mouse IgG, Alexa 555 labelled donkey anti-rabbit IgG, Annexin V-FITC Apoptosis Detection Kit, Cell Cycle and Apoptosis Analysis Kit and Cell Counting Kit-8 were all purchased from Beyotime Institute of Biotechnology. Mouse TNF-alpha and interleukin-12/P70 ELISA kits were purchased from BioLegend, Inc. and Beijing Huabo Deyi Biotechnology Co., Ltd, respectively. All other reagents were obtained from Sinopharm Chemical Reagent Co., Ltd.

Cy3-siRNA was purchased from Guangzhou RiboBio Co., Ltd. FAM-siRNA, Scrambled siRNA and CDK1-siRNA were synthesized and purified with HPLC by Shanghai GenePharma Co. Ltd. CDK1-siRNA (5'-GGAACUUCGUCAUCCAAAUTT-3') for both *in vitro* and *in vivo* transfections was designed for targeting human CDK1. Fluorescence labeled siRNA molecules were used for flow cytometry and intracellular tracing. Scrambled siRNA molecules were used for nanoparticle characterization and *in vitro* safety study.

Detailed synthesis procedure of DC. DC was synthesized through five steps (Figure S1). First, di-tert-butyl dicarbonate, triethylamine were added to the solution of 3-amino-1, 2-propanediol (3:3:2, molar ratio) in chloroform and methanol (v/v, 1:1) under argon atmosphere. The reaction mixture was stirred for 4 h at room temperature to obtain amino protected 3-amino-1, 2-propanediol. Then, a solution of oleoyl chloride in dichloromethane was dropwise added to a solution of amino protected 3-amino-1, 2-propanediol (1:3, molar ratio to oleoyl chloride) and triethylamine in dichloromethane, the reaction mixture was stirred for 20 h at room temperature under nitrogen atmosphere. The organic phase was extracted with distilled water and evaporated. The residue was purified with silica gel column chromatography. Trifluoroacetic acid was added to the above product in dichloromethane and stirred at room temperature for 4 h. Add saturated $NaHCO_3$ to the solvent and extract the product with ethyl acetate. The organic phase was evaporated to afford DOA (dioleoyl ethanolamine). The mixture of DOA and citraconic anhydride (1:1.2, molar ratio) dissolved in chloroform and triethylamine was stirred at room temperature for 3

h, and the product was purified with recrystallization to get DC. All the compounds were dissolved in $CDCl_3$ and analyzed by 400Hz ^1H NMR spectroscopy (Bruker Avance III 400 Spectrometer).

Preparation and characterization of DCLC nano-Transformers. DCLC nano-Transformers were prepared using probe ultrasonic technique. Ternary phase diagram was built to obtain the most suitable ratio of the components to form liquid crystalline nanoparticles. Various ratios of DC, PBS and oleic oil were added into centrifuge tube, well mixed and incubated at 37 ^oC for 30 min. Then the obtained systems were sonicated at 1% power for 10 seconds using the probe ultrasonicater (Scientz-IID, Ningbo scientz biotechnology Co., Ningbo, China). Polarized mode of the Leica DMI4000B microscope was used to examine the formation of nano-Transformers. Material ratios with rod-like polarized pattern were marked as nano-Transformers growth.

For formulation optimization, siRNA loaded DCLC nano-Transformers with different material ratios (volume ratios of DC/pH 7.4 PBS/oleic oil = 8/11/1, 10/9/1, 12/7/1, 14/5/1, 16/3/1 and 18/1/1) were prepared. Briefly, DC was well mixed with PBS (containing siRNA) and oleic oil, and incubated at 37 ^oC for 30 min. Then the obtained systems were diluted 2 times with PBS and sonicated at 1% power for 50 seconds to form the siRNA loaded DCLC nano-Transformers. siRNA loaded DCLC nano-Transformers were diluted with PBS and added on a 2% agarose gel prepared in TBE buffer. Electrophoresis was performed at 50 V during 1 h. siRNA strips were observed with BioRad Gel Doc™ XR imaging system.

To evaluate the stability of DCLC nano-Transformers, DC/PBS/oleic oil = 16/3/1 was used to prepare siRNA loaded DCLC nano-Transformers. For dilution stability assay, DCLC nano-Transformers were diluted into final concentration of 6, 0.6, 0.06 and 0.006 mg/mL using pH 7.4 PBS containing 10% fetal bovine serum. Samples were incubated at 37 ^{o}C for 30 min. Hydrodynamic size and zeta potential were measured by dynamic light scattering using a Malvern Zetasizer Nano ZS. For serum stability assay, siRNA loaded DCLC nano-Transformers were diluted 2 times with fetal bovine serum followed by incubating at 37 ^{o}C for various time periods (0, 2, 4, 6, 8, 10 and 12 hours). At selected time points, samples were immediately stored at -80 ^{o}C to stop the degradation. Triton X-100 was then added to the incubation mixture to extract residual siRNA from nanoparticles. Subsequently, samples were loaded on a 2% agarose gel, and electrophoresis was performed as previous.

To evaluate the transformation behavior of siRNA loaded DCLC nano-Transformers, DCLC nano-Transformers were dispersed into 10-fold-volume pH 5.0 PBS and incubated at 37 ^{o}C for 2 hours. At selected time points, 0.1 M NaOH with 1 mg/mL fluorescamine was used to adjust pH to 8.0 to stop the transformation and label DOA. Samples were then observed under a confocal microscope (Olympus FV 1000) to reveal the direct transformation process. Hydrodynamic size and zeta potential were measured by dynamic light scattering using a Malvern Zetasizer Nano ZS. Morphology change was assessed using both SEM (Phenom ProX) and Cryo-FESEM (Hitachi S-4800).

The crystal lattice changing was determined using small angle X-ray scattering (SAXS). To

eliminate the influence of siRNA structure on SAXS curves, empty DCLC nano-Transformers prepared at material volume ratio of DC/pH 7.4 PBS/oleic oil = 16/3/1 were used. DCLC nano-Transformers were dispersed into 10-fold-volume pH 5.0 PBS and incubated at 37 ^{o}C for several time periods (0, 30, 60 and 90 min). At selected time points, samples were prepared in quartz capillaries (Hilgenberg Glas, Germany). SAXS experiments were performed at beamline BL16B1 of the Shanghai Synchrotron Radiation Facility in China. 2D diffraction data were acquired by the detector at a sample-to-detector distance of 1.78 m with an X-ray wavelength of 1.24 Å. Background scattering due to the solvent was subtracted. Data were then integrated into the one-dimensional scattering function *I(q)* using FIT2D software.

^{1}H NMR spectrum was used to determine the lipid constituent in DCLC nano-Transformers. DCLC nano-Transformers were prepared with DC and water to eliminate the influence of phosphate and oleic oil on ^{1}H NMR spectrum. DCLC nano-Transformers were dispersed into 10-fold-volume pH 5.0 PBS and incubated at 37 ^{o}C for 2 h. Sample before incubation was directly transferred into round-bottom flasks. Water was then removed from the system by rotary evaporating. Sample after incubation was water-removed and additionally purified to get the lipid material. The remainders of both samples were dissolved in CDCl3 and analyzed by 400Hz 1H NMR spectroscopy.

Cell viability and ATP level analysis. HepG2 cells were seeded in a 96-well plate (1,000 cells per well) and cultured overnight, after which they were incubated with scrambled

siRNA loaded nano-Transformers and Lipo 2000 at varying siRNA concentration at 37 °C for 24 h. After incubation, the cell morphology was observed using confocal microscopy. Cell viability and cellular ATP level were determined using Cell Counting Kit-8 and ATP detection kit as described by the manufacturer's instructions.

Cellular uptake and intracellular siRNA distribution study. For cellular uptake analysis, HepG2 cells were seeded into 12-well plates (1.0×10^5 cells per well) and cultured overnight. Cells were then incubated with different formulations containing FAM-siRNA (working concentration 100 nM) for 30 min, and lifted with dissociation buffer. The level of nanoparticle uptake was determined using a BD Bioscience FACScalibur flow cytometer. Mean fluorescence intensity of each group was analyzed using FlowJo 7.6.1 software. To study the intracellular distribution of the siRNA molecules, HepG2 cells were seeded in a 24-well plate containing circle glass cover slides (3×10^4 cells per well) for 24 h. Then the cells were treated with different formulations at FAM-siRNA concentration of 100 nM. If needed, bafilomycin A1 (working concentration 100 nM) was added into the culture medium at least 1 h before the formulations. After incubation for 30 min and 120 min, immunofluorescent staining of both early and late endosomes were performed by using purified mouse anti-EEA1 and LAMP1 rabbit mAb primary antibodies, Alexa 555 labeled donkey anti-mouse IgG and Alexa 555 labeled donkey anti-rabbit IgG as secondary antibodies, respectively. Cell nucleus were stained by DAPI. Confocal microscopy (Olympus FV 1000) and STED microscopy (Leica TCS SP8 STED 3X) were used to

observe the fluorescent signals. Pearson's coefficiency was calculated using the JACoP plugin of ImageJ 1.46r software. In addition, to validate the distinction between free siRNA and nanoparticle-condensed siRNA observed in cells, Alexa 647 labeled siRNA solution, siRNA containing DCLC nano-Transformers or Lipo 2000, as well as siRNA containing nanoparticles that incubated with isolated lysosomes were observed under the Olympus FV 1000 microscope.

Endosomal escape process and mechanism study. Time-lapse fluorescence microscopy was used to investigate the dynamic endosomal escape process of siRNA loaded nanocarriers. Spin-disk confocal microscope can generate images in a much faster way than laser scanning confocal microscope, leading to the minimal photobleaching of fluorescent signals, and is suitable for long-time live-cell fluorescence imaging. HepG2 cells were seeded on Ibidi 8-well chamber slide at a density of 5,000 cells per well and cultured at 37 ^{o}C for 24 h. Cells were incubated with Hoechst 33258 (10 μg/mL) for about 15 min to stain the cell nucleus. Afterwards, cells were washed twice using PBS and then incubated with Alexa-647 labeled dextran (1 mg/mL) and siRNA loaded nano-Transformers or Lipo 2000 with siRNA concentration of 100 nM for another 10 min. Finally, cells were washed, incubated with fresh medium and then observed under a spin-disk confocal microscope (Zeiss Cell Obsever SD). For the proton inhibited group, bafilomycin A1 (working concentration 100 nM) was added to the culture medium at least 1 h before the addition of nano-Transformers. Fluorescent images of nano-carriers, siRNA and endosomes containing

dextran were taken every 10 seconds. Integrated density of siRNA and dextran fluorescent dot in each image was analyzed with ImageJ 1.46r software.

The interaction between siRNA loaded nanoparticles and model endosomal membrane was observed to study the mechanism of endosomal escape. DiO-labeled nano-Transformers or Lipo 2000 were encapsulated into the model endosomes using a thin-film hydration method. In detail, the nanoparticles were firstly suspended in pH 5.0 or pH 7.4 PBS, which were used to imitate the acidic endosomal environment and the proton pump inhibited situation, respectively. The obtained solution was then added to the DiI-labeled DOPC thin film (to simulate the endosomal membrane) and hydrate at room temperature for 5 min using a rotary evaporator. Next, the system was transferred to centrifuge tube and immediately incubated at 37 °C in a water bath kettle and assessed using Leica fluorescence microscopy (DMI4000B) at each time point.

FRET was used to directly study the fusion between nanoparticles and the lysosome membrane. In detail, HepG2 cells were disrupted at 4 °C using an APV 2000 high pressure homogenizer. Lysosomes were then isolated from HepG2 cells by differential centrifugation according to the reported research[1] and lifted using pH 5.0 PBS. Isolated lysosomes were labeled using DiI and siRNA containing nano-Transformers or Lipo 2000 were labeled using DiO, respectively. Nanoparticles were then mixed with equal weight of lysosome and incubated at 37 °C. Fluorescence emission spectrum of the system during 480-700 nm was measured at selected time points with excitation of 440 nm using the BioTek Synergy H1

microplate reader.

Computer simulation of detailed molecular dynamic mechanism in endosomal escape.

To further study the detailed molecular dynamic endosomal escape mechanism of DCLC nano-Transformers, the lipid bilayer was built by Charmm-GUI online[2-5] using computer simulation. Each layer contained 25 DOPC molecules and 750 water molecules. As for the DC and DOA molecules, the structures were optimized by Gaussian09[6] package at the level of B3LYP/6-31g*. Then the partial atomic charges of these molecules were calculated by the restrained electrostatic potential (RESP)[7] charge from the calculation with Gaussian09 package at HF/6-31g* level. The AMBER Lipid14 force field[8] was applied to the DOPC molecules and the AMBER GAFF force field[9] to the DC or DOA molecules. Finally, the topology files and the initial coordinates were generated by the *tleap* program in Ambertool14[10]. All the Molecular dynamics were completed by the *sander* program in AMBER12[11]. Prior to the heating molecular dynamic simulations, 100 thousand steps minimization, including 40 thousand steps conjugate gradient iterations and 60 thousand steps steepest descent energy minimization, were carried out in order to optimize the initial structures. After the optimization, each system was heated up from 0 K to 300 K gradually under the NVT ensemble for 150 ps. Then, 1 ns molecular dynamic simulations were performed under NPT ensemble. During the molecular dynamic simulations, the SHAKE algorithm[12] was employed to constrain all hydrogen-containing bonds with a tolerance of 10^{-5}. The periodic boundary condition was kept and a cutoff of 8 A was set for both van der

Waals and electrostatic interactions. Finally, another at least 80 thousands minimization with the convergence of 10^{-5} were performed for every system in order to get the final energy value.

***In vitro* transfection efficiency and cytotoxicity.** For cell cycle and apoptosis analysis, HepG2 cells were seeded into 12-well plates (1.0×10^5 cells per well) and cultured overnight. 100 μL of PBS, CDK1-siRNA loaded nano-Transformers, CDK1-siRNA loaded Lipo 2000 or scrambled siRNA loaded nano-Transformers was diluted into 1 mL using complete DMEM and was used to replace the culture medium. After incubating for 36 h, cells were lifted with dissociation buffer, then stained according to the manufacturer's instructions of Annexin V-FITC Apoptosis Detection Kit and Cell Cycle and Apoptosis Analysis Kit. Acquisition was performed using a BD Bioscience FACScalibur flow cytometer. Data of each group was analyzed using FlowJo 7.6.1. Cytotoxicity of these formulations was evaluated using the MTT assay. HepG2 cells were seeded in 96-well plates at 5,000 cells per well and cultured overnight. The cells were then incubated with different formulations (CDK1-siRNA concentration 100 nM) for 48 h. PBS diluted with DMEM was set as negative control group. The MTT reagent was added to each well and incubated for another 4 h. After removal of the medium, 200 μL of DMSO was added to each well and the absorbance at 490 nm was measured by a microplate reader (BioTek Synergy H1, USA). The cell viability was calculated.

Quantitative PCR. Total RNA was extracted from cells or tumors using TRIzol reagent (Invitrogen) according to the manufacturer's instructions. 500 ng of total RNA was used to reverse transcription using the PrimeScriptTM RT Reagent Kit (Takara). The quantitative PCR was performed using SYBR® Premix Ex Taq^{TM} II (Takara). The average threshold cycle for each gene was determined from triplicate reactions, and the expression level was normalized to GAPDH. The primers used for detecting the expression levels of CDK1 and GAPDH were as follows: CDK1-F: 5'-CAG GAT GTG CTT ATG CAG GA-3', CDK1-R: 5'-CCA CAA AAT GCA GGG ACT TC-3', GAPDH-F: 5'-CAT GGC CTT CCG TGT TCC TA-3', GAPDH-R: 5'-CCT GCT TCA CCA CCT TCT TGA T-3'.

Western blotting. HepG2 cells treated with different formulations were lysed using RIPA buffer with protease inhibitor. Equal amounts of total protein lysate were denatured in Laemmeli buffer at 70 °C for 5 min, separated by a 7% SDS-PAGE and transferred to PVDF membranes. Anti-CDK1 antibody and Anti-beta Actin antibody were used at a 1:1000 dilution in 5% milk. The proteins were detected using an ECL detection system (Perkin-Elmer) according to the manufacturer's instructions.

***In vivo* antitumor efficacy and safety study.** Balb/c nude mice and ICR mice were obtained from Shanghai Lab. Animal Research Center. All animal experiments were performed in accordance with NIH guidelines and approved by the Institutional Animal Care and Use Committee at Shanghai Institute of Materia Medica (IACUC number:

2016-06-GY-24). For *in vivo* antitumor efficacy study, tumor-bearing mice were established by subcutaneous inoculation of HepG2 cell suspension (1.0×10^6 cells in 100 μL fetal bovine serum free DMEM) into axilla of male Balb/c mice. The tumors were allowed to grow to a size of 50~100 mm^3. The mice were then randomly divided into 4 groups. CDK1-siRNA loaded DCLC nano-Transformers, scrambled siRNA loaded DCLC nano-Transformers, CDK1-siRNA loaded Lipo 2000 or PBS was peritumorally injected every other day at a siRNA dose of 20 μg per mice. Tumor size (volume = (length × $width^2$)/2) was monitored over time. At day 21 after start of treatment, mice were euthanized and tumor growth inhibition was calculated as (1 – TVt/TVc) × 100%, where TVt and TVc were the mean tumor volume of treated and control groups, respectively. The tumor tissues were excised, sectioned and then stained with hemoxylin and eosin (H&E) for histological analysis.

To investigate the siRNA distribution in tumor tissues, tumor-bearing Balb/c mice were established as previously mentioned. Nano-Transformers and Lipo 2000 containing FAM-siRNA were intratumorally injected into mice with a siRNA dose of 20 μg per mice. Tumor tissues were then collected 4 h after injection, and cut into 7-μm-thick sections using a Leica 2800 Frigocut-E slicer. Tissue samples were then fixed and the immunofluorescent staining procedure as mentioned in intracellular siRNA distribution study was followed. Confocal microscopy (Olympus FV 1000) was used to observe the fluorescent signals. Intracellular distribution of the siRNA molecules was analyzed using ImageJ 1.46r

software.

ICR mice were used for investigating the IL-12 and TNF-α levels after intravenous injection. 24 h following tail vein injection of different formulations, blood serum was collected and used for ELISA of mouse TNF-α and IL-12 using the Mouse TNF-alpha and interleukin-12/P70 ELISA kits according to the manufacturer's instructions.

Statistical analysis. Significant differences were evaluated using an independent-samples *t* test or Wilcoxon rank test, except that multiple treatment groups were compared within individual experiments by the ANOVA test. The Chi-square test was used for contingency table analysis. Values of *p* less than 0.05 were considered significant. All values were presented as mean ± SD.

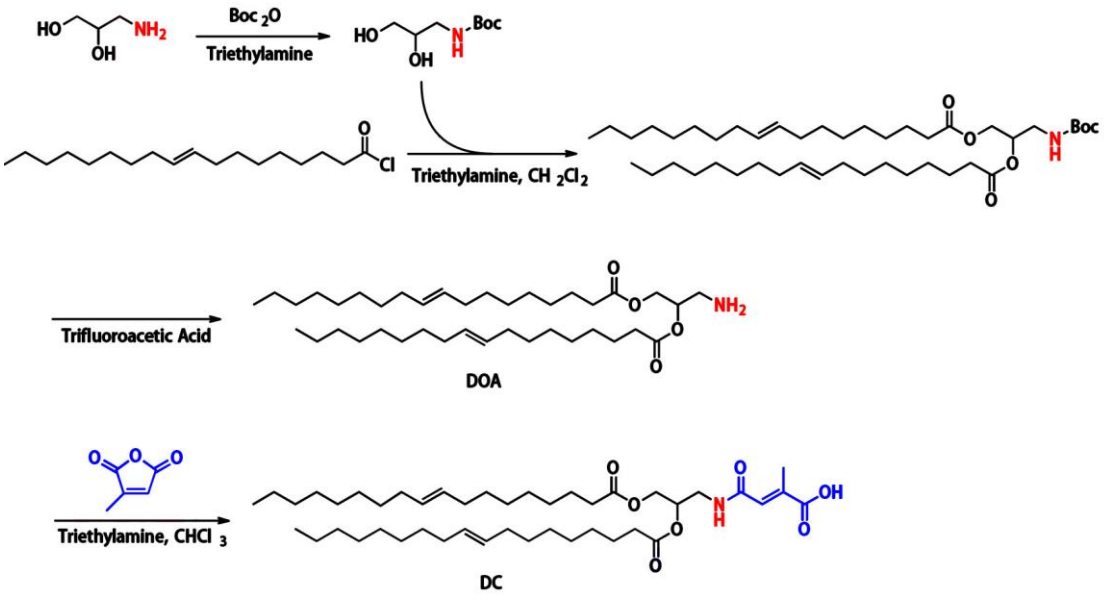

Figure S1. The synthesis procedures of DOA and DC.

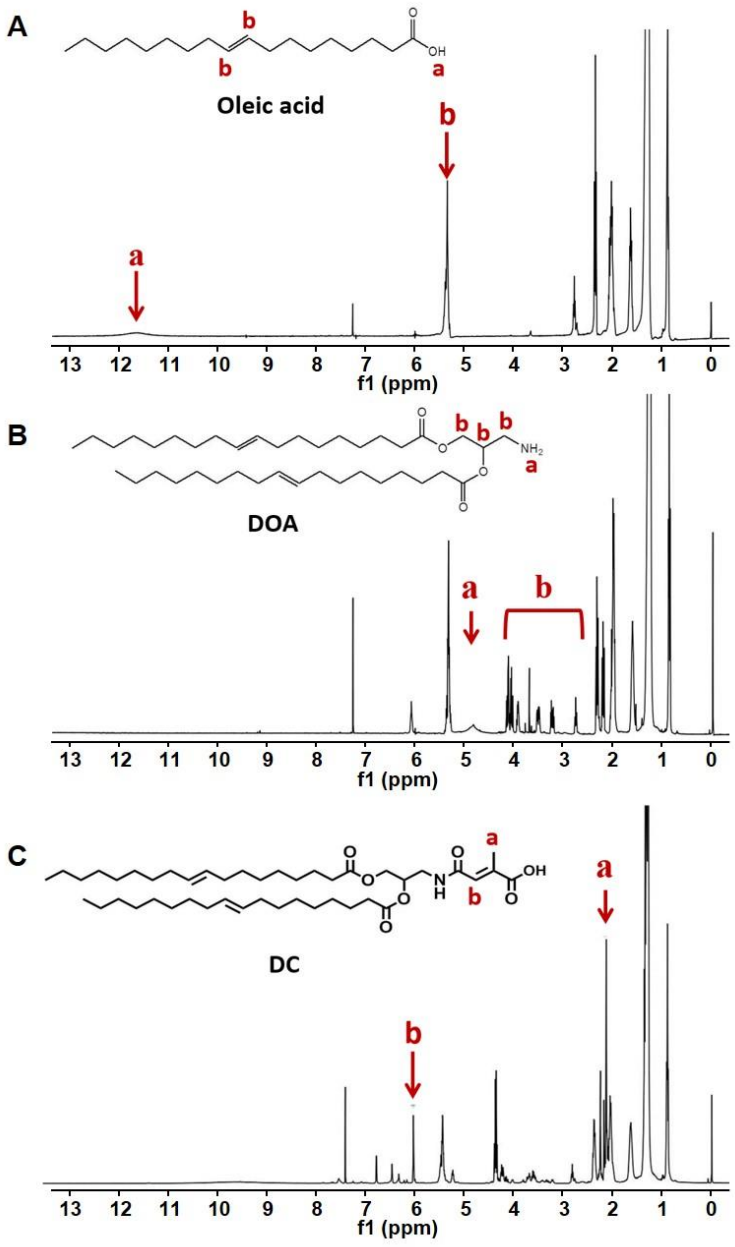

Figure S2. ^{1}H NMR spectra ($CDCl_3$, 400 MHz) of the Oleic acid (A), DOA (B) and DC (C). Comparing the spectrum of DC to oleic acid and DOA, the characteristic ^{1}H NMR peak of olefinic bond (-CH=CH-) at δ=5.4 ppm and frame structure of 3-amino-1,2-propanediol at 2.7-4.1 ppm were present. In addition, the peak of amino at δ=4.8 ppm disappeared, and two

important peaks were observed, including methyl group and olefinic bond of citraconic acid at δ=2.1 ppm and 6.1 ppm. Data verified that DC was successfully constructed by the reaction of the amino group of DOA with citraconic anhydride.

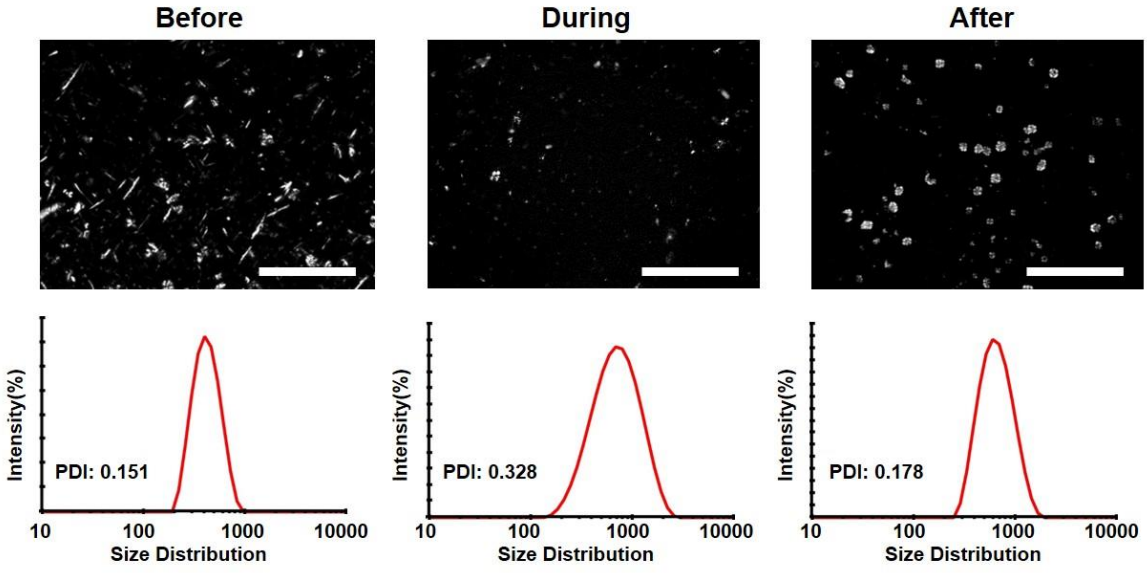

Figure S3. Polarized microscopy image and size distribution of DCLC nano-Transformers before (pH 7.4 PBS), during (pH 5.0 PBS) and after (pH 5.0 PBS) transformation. During the transformation process, PDI increased and the polarizing signal decreased. These results demonstrated that DCLC nano-Transformers were going through an amorphous and chaotic state. Scale bar = 5 μm.

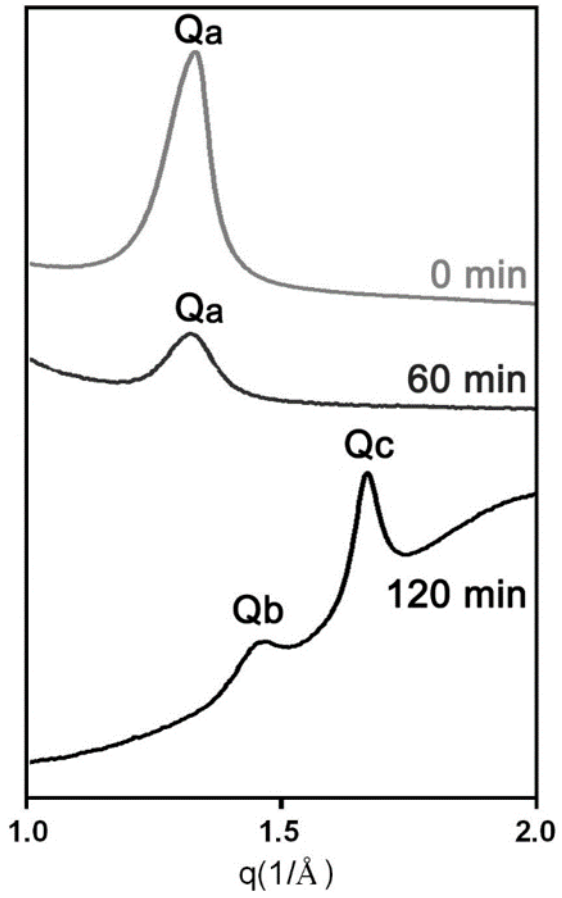

Figure S4. SAXS data for DCLC nano-Transformers incubating with pH 6.0 PBS for 0 min, 60 min and 120 min, respectively. The transformation of DCLC nano-Transformers still occured under this condition but slower than incubating with pH 5.0 PBS.

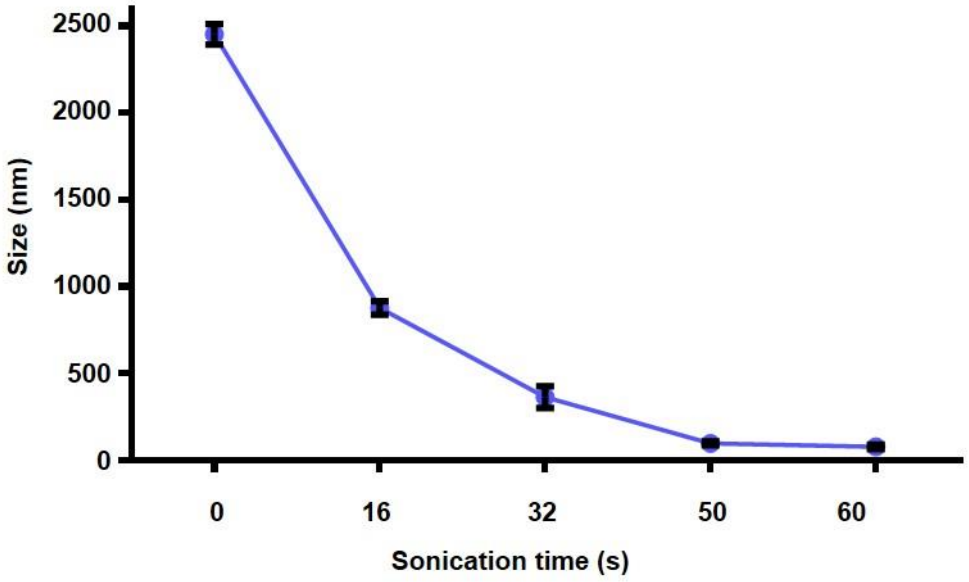

Figure S5. Size of DCLC nano-Transformers changed along with sonication.

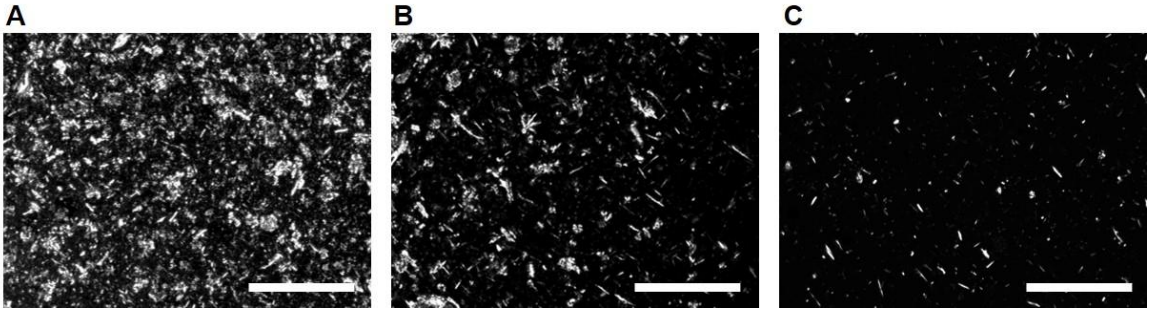

Figure S6. Polarized microscopy images of DCLC nano-Transformers in serum containing pH 7.4 PBS solution at concentrations of 6000 mg/L (A), 600 mg/L (B) and 60 mg/L (C). The polarized pattern during dilution showed no visible difference. Scale bar = 5 μm.

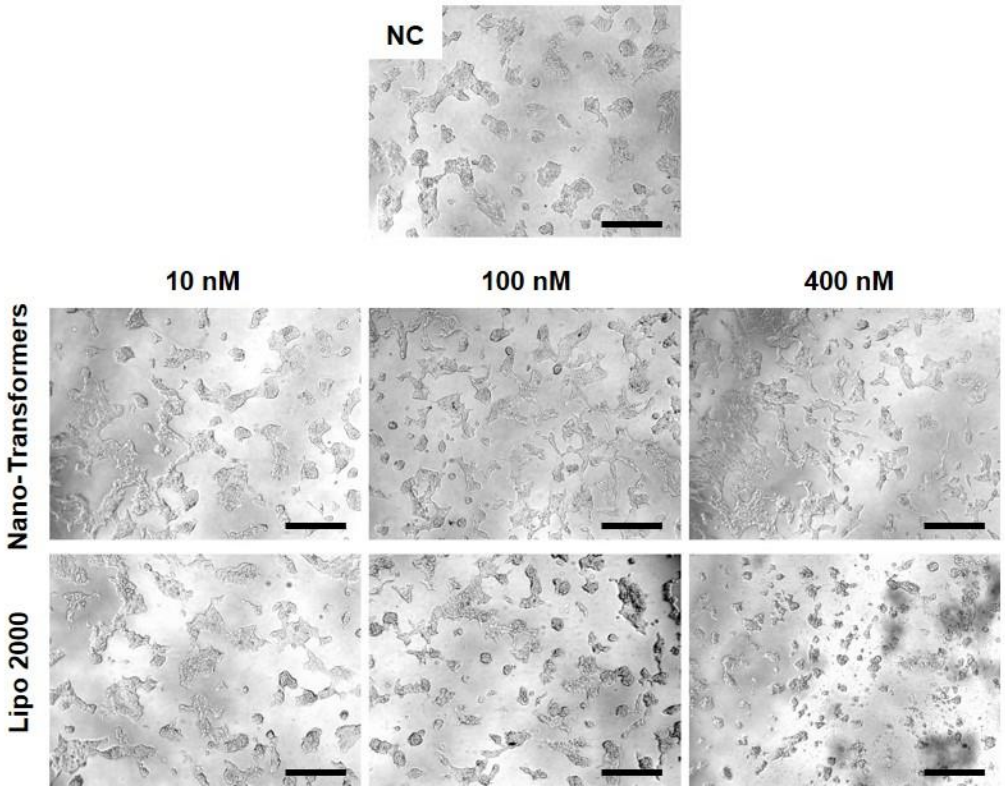

Figure S7. DIC images of HepG2 cells incubated with scrambled siRNA loaded DCLC nano-Transformers or Lipo 2000 at siRNA concentration of 10 nM, 100 nM and 400 nM, respectively. High concentration of Lipo 2000-siRNA nanoparticle induced remarkable cellular morphology change while the DCLC nano-Transformer group always remaining the same, indicating the DCLC nano-Transformers were much safer than Lipo 2000. Scale bar = 100 μm.

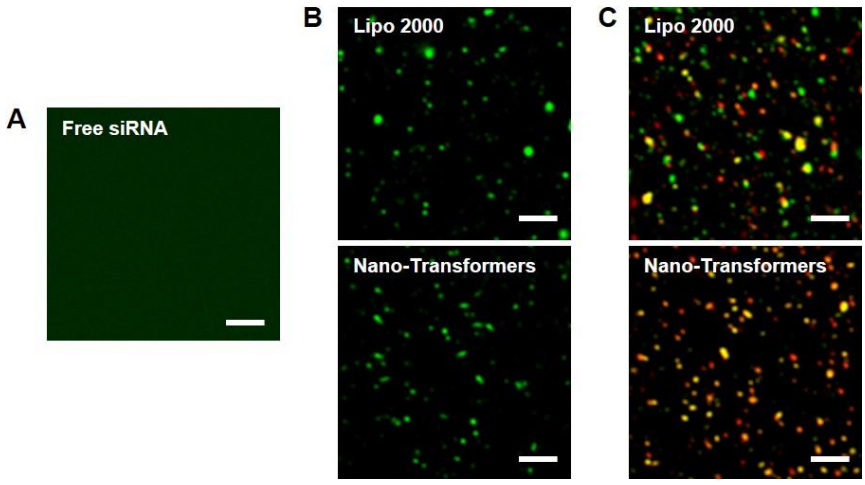

Figure S8. Confocal images of siRNA molecules at different conditions. Free siRNA molecules showed well-distributed green signals (A). When encapsulated into nanocarriers (Lipo 2000 or nano-Transformers), siRNA signals showed green bright spots before (B) and after (C) incubating with isolated lysosomes (red) at 37 °C for 1 h. Scale bar = 2 μm.

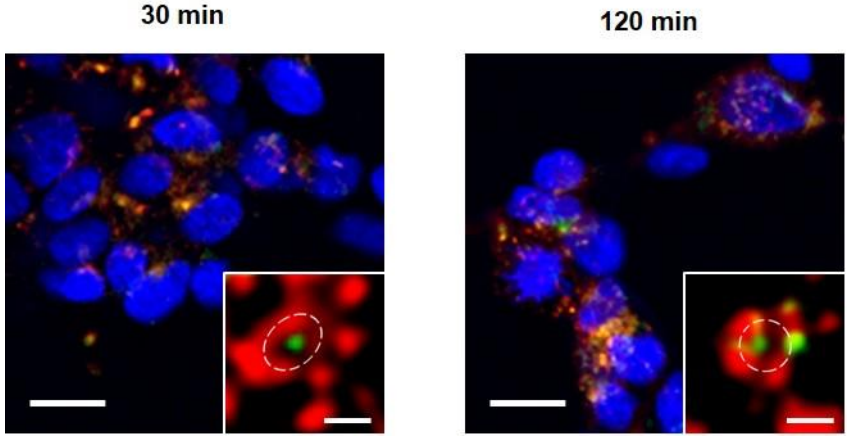

Figure S9. Confocal and SRM images of DCLC nano-Transformers treated HepG2 cells with the presence of bafilomycin A1, showing the relative localization of the Alexa

555-labeled endosome (red) and the FAM-siRNA (green) at incubation time of 30 min and 120 min, respectively. Cell nuclei were stained with DAPI (blue). Scale bar = 30 μm. SRM images of magnified endosomes are shown as insertion. Scale bar = 200 nm.

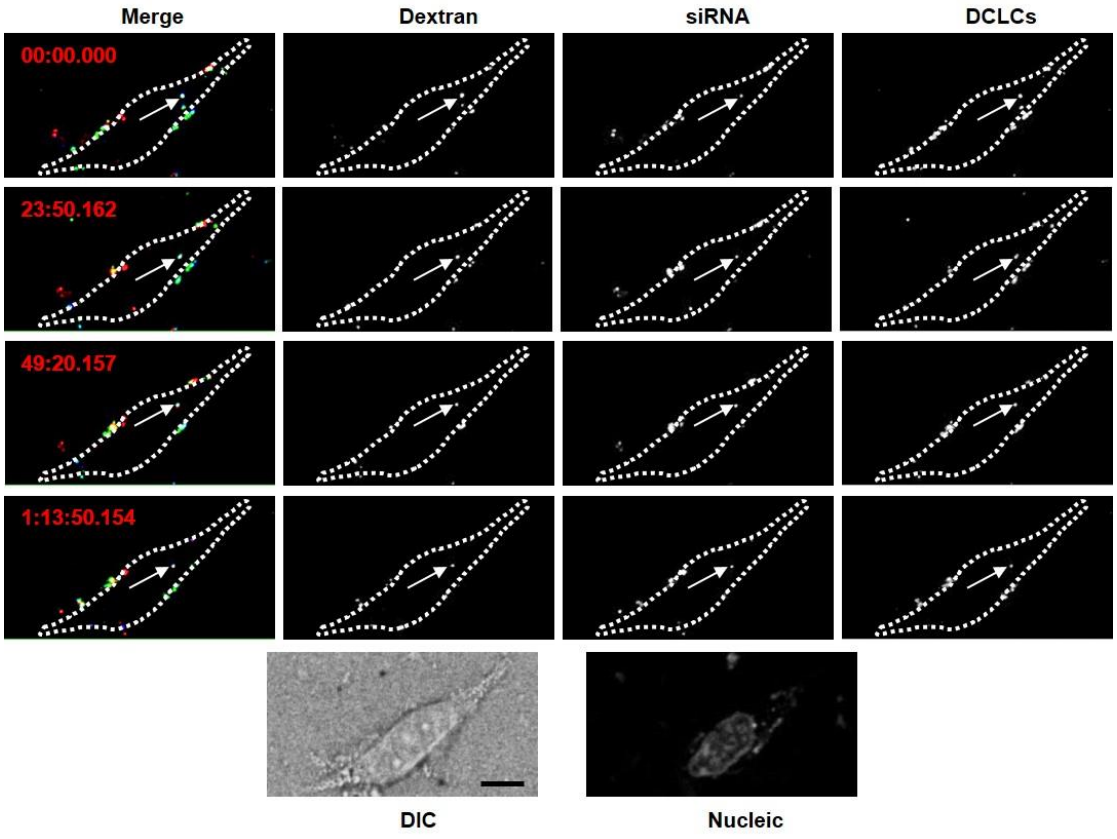

Figure S10. Spinning-disk confocal microscopy images of DCLC nano-Transformers treated HepG2 cells with the presence of bafilomycin A1. Endosomes were labeled by Alexa 647-Dextran (blue). siRNA was labeled by Cy3 (red). Nanoparticles were labeled by DiO (green). Scale bar = 10 μm.

REFERENCES

1. Wieckowski, M. R.; Giorgi, C.; Lebiedzinska, M.; Duszynski, J.; Pinton, P. *Nat Protoc* **2009,** 4, (11), 1582-90.
2. Jo, S.; Kim, T.; Iyer, V. G.; Im, W. *J Comput Chem* **2008,** 29, (11), 1859-65.
3. Jo, S.; Lim, J. B.; Klauda, J. B.; Im, W. *Biophys J* **2009,** 97, (1), 50-8.
4. Wu, E. L.; Cheng, X.; Jo, S.; Rui, H.; Song, K. C.; Davila-Contreras, E. M.; Qi, Y.; Lee, J.; Monje-Galvan, V.; Venable, R. M.; Klauda, J. B.; Im, W. *J Comput Chem* **2014,** 35, (27), 1997-2004.
5. Lee, J.; Cheng, X.; Swails, J. M.; Yeom, M. S.; Eastman, P. K.; Lemkul, J. A.; Wei, S.; Buckner, J.; Jeong, J. C.; Qi, Y.; Jo, S.; Pande, V. S.; Case, D. A.; Brooks, C. L., 3rd; MacKerell, A. D., Jr.; Klauda, J. B.; Im, W. *J Chem Theory Comput* **2016,** 12, (1), 405-13.
6. Frisch, M.; Trucks, G.; Schlegel, H.; Scuseria, G.; Robb, M.; Cheeseman, J.; Scalmani, G.; Barone, V.; Mennucci, B.; Petersson, G., Gaussian 09, revision D. 01. Gaussian, Inc., Wallingford CT: 2009.
7. Bayly, C. I.; Cieplak, P.; Cornell, W.; Kollman, P. A. *The Journal of Physical Chemistry* **1993,** 97, (40), 10269-10280.
8. Dickson, C. J.; Madej, B. D.; Skjevik, A. A.; Betz, R. M.; Teigen, K.; Gould, I. R.; Walker, R. C. *J Chem Theory Comput* **2014,** 10, (2), 865-879.
9. Wang, J.; Wolf, R. M.; Caldwell, J. W.; Kollman, P. A.; Case, D. A. *J Comput Chem* **2004,** 25, (9), 1157-74.
10. Case, D.; Darden, T.; Cheatham III, T.; Simmerling, C.; Wang, J.; Duke, R.; Luo, R.; Walker, R.; Zhang, W.; Merz, K. *There is no corresponding record for this reference*.
11. Case, D. A.; Cheatham, T. E., 3rd; Darden, T.; Gohlke, H.; Luo, R.; Merz, K. M., Jr.; Onufriev, A.; Simmerling, C.; Wang, B.; Woods, R. J. *J Comput Chem* **2005,** 26, (16), 1668-88.
12. Ryckaert, J.-P.; Ciccotti, G.; Berendsen, H. J. *Journal of Computational Physics* **1977,** 23, (3), 327-341.